Integrative Biology

PAPER

Probing bacterial–fungal interactions at the single cell level†

Cite this: *Integr. Biol.*, 2014, 6, 935

Claire E. Stanley,‡[a] Martina Stöckli,‡[b] Dirk van Swaay,[a] Jerica Sabotič,[c] Pauli T. Kallio,[b] Markus Künzler,[b] Andrew J. deMello*[a] and Markus Aebi*[b]

Received 4th July 2014,
Accepted 9th August 2014

DOI: 10.1039/c4ib00154k

www.rsc.org/ibiology

Interactions between fungi and prokaryotes are abundant in many ecological systems. A wide variety of biomolecules regulate such interactions and many of them have found medicinal or biotechnological applications. However, studying a fungal–bacterial system at a cellular level is technically challenging. New microfluidic devices provided a platform for microscopic studies and for long-term, time-lapse experiments. Application of these novel tools revealed insights into the dynamic interactions between the basidiomycete *Coprinopsis cinerea* and the bacterium *Bacillus subtilis*. Direct contact was mediated by polar attachment of bacteria to only a subset of fungal hyphae suggesting a differential competence of fungal hyphae and thus differentiation of hyphae within a mycelium. The fungicidal activity of *B. subtilis* was monitored at a cellular level and showed a novel mode of action on fungal hyphae.

Insight, innovation, integration

The integration of microfluidic platforms with a growing filamentous mycelium and bacteria opens a great potential for interaction analysis. Currently, no method exists that enables the *dynamic* interactions between filamentous fungi and bacteria to be monitored at the single cell level and in real-time. The confinement provided by the bacterial–fungal interaction device enables the spatiotemporal fingerprints of bacterial–fungal associations to be assessed. In contrast, our exchange device enables the fluidic environment surrounding hyphae to be manipulated. Together, these devices provide a novel means to assess and dissect these complex relationships at the single cell level and have revealed novel insights into the interaction of *Bacillus subtilis* with *Coprinopsis cinerea*, such as bacteria-induced blebbing of hyphal cells and dynamic polar attachment.

Introduction

Bacteria and fungi often share the same habitat and their interactions can have major implications on the biology of the partners involved and on the respective environment.[1–5] These microorganisms are found closely associated in environmental samples, with bacteria attaching to fungal hyphae.[6] Dung of herbivorous animals, as an example, is a nutrient-rich environment where bacteria and fungi interact and compete for resources.[7] Fungi and bacteria share a lifestyle of nutrition by absorption and thus antagonistic strategies have evolved in both clades due to this trophic competition.[8] From such strategies, important applications in the medical and agricultural sciences have emerged; for example, antibacterial secondary metabolites and peptides from fungi are used as antibiotics[9–11] and different bacterial species are studied as biological control agents in agriculture against plant pathogenic fungi.[12–15] Due to technical limitations, dynamic bacterial–fungal interactions (BFIs) at the single cell level are not well studied. As such, there is a need for the development of new technological platforms to interrogate and quantify these complex and dynamic interactions, presenting opportunities to gain insights into the phenotypic heterogeneities and spatial organisations of mixed microbial communities, for example.

Traditional approaches for exploring interactions between fungi and bacteria are based on confrontation assays, where axenic fungal and bacterial inocula are introduced onto solid or into liquid media, incubated together for a period of time and the growth of the interacting species measured.[13,16] These assays monitor BFIs at the macroscopic level, *e.g.* by growth inhibitions. However, such measurements yield limited information at the cellular level, since specific interactions between hyphae and bacteria and their spatial organisation cannot easily be monitored.

[a] *Institute for Chemical and Bioengineering, Department of Chemistry and Applied Biosciences, ETH Zürich, Vladimir-Prelog-Weg 1, CH-8093 Zürich, Switzerland. E-mail: andrew.demello@chem.ethz.ch*

[b] *Institute of Microbiology, Department of Biology, ETH Zürich, Vladimir-Prelog-Weg 4, CH-8093 Zürich, Switzerland. E-mail: markus.aebi@micro.biol.ethz.ch*

[c] *Department of Biotechnology, Jožef Stefan Institute, Jamova 39, SI-1000 Ljubljana, Slovenia*

† Electronic supplementary information (ESI) available. See DOI: 10.1039/c4ib00154k

‡ These authors contributed equally to this work.

Downloaded from https://academic.oup.com/ib/article-abstract/6/10/935/5199045 by ETH Zürich user on 21 February 2019

Assays using multi-well plates[14] provide one approach for obtaining information at the microscopic level. However, high-resolution imaging, hyphal tracking and media exchange are challenging in such a setup. Conventional microscopic imaging, where hyphae are grown on microscopy slides coated with agar,[17] for example, are also subject to similar drawbacks, particularly in the sense that it is difficult to monitor dynamic interactions in real time due to the lack of confinement. Currently, there are few tools that allow the control of environmental conditions in a precise and dynamic manner and, at the same time, the monitoring of interactions at a microscopic level.

Microfluidics describes the use of engineered systems, possessing micron-scale features, to control, manipulate and analyse pL–μL fluid volumes.[18] Originally developed for use in the chemical sciences, microfluidic devices have been shown to provide a platform for enhanced analytical performance,[19] high-throughput experimentation[20] and controlled generation of chemical gradients,[21] for example. In recent years, the use of microfluidic systems in the microbiological sciences has grown apace, owing to the ease of manipulation of microorganisms on a single cell basis and the ability to control microenvironments in a rapid and precise manner.[22] Importantly, the use of microfabrication techniques for the rapid and inexpensive production of microfluidic devices allows bespoke systems to be designed for the problem at hand, unlocking new experimental opportunities for microbiologists. The polymer, poly(dimethylsiloxane) (PDMS), is an ideal substrate material for use in biological applications, having desirable physical and chemical properties.[23] Importantly, this elastomeric polymer is permeable to gases, enabling experiments to be conducted in an aerobic environment, and allows optical detection from 240 to 1100 nm.[24]

Methods currently available for processing live microorganisms-on-a-chip are most frequented by technologies that explore bacterial microenvironments. As summarised by Wessel *et al.*,[25] the main advantages afforded by these studies include the ability to confine cells, where the influence of spatial structure on the behaviour of bacterial cells can be examined,[26] and detect small molecules, leading to a better understanding of the composition and variation in the microenvironment.[27] As a result, light has been shed on a variety of topics including bacterial chemotaxis,[28] phenotypic heterogeneity in populations of bacteria[29] and quorum sensing.[30] Studies utilising filamentous fungi in microfluidic devices have emerged only very recently, with a clear focus on probing the growth dynamics of filamentous fungi using microfabricated structures.[31] Microfluidic technologies entertaining mixed microbial populations, such as the microfluidic droplet platform described by Park *et al.*[32] for detecting symbiotic relationships in communities comprised of multiple populations of bacteria, are rare and, at present, no method exists that enables dynamic interactions between bacteria and filamentous fungi to be monitored using microfluidic platforms at the cellular level and quantified in real-time. Further, it is not possible to exchange media surrounding hyphae and monitor their response in a controlled manner using conventional methods; such a feat would add a significant new dimension to the mycological toolbox.

To address the aforementioned needs, we present a novel microfluidic platform that enabled BFIs to be probed and fluid exchange to be performed in a controlled and rapid manner. The first microfluidic device allows confrontations between bacteria and fungi in a confined environment. A key feature of this device, when compared to macroscale systems, is the confinement of submerged hyphae (defined by the height of the microchannel) to a single layer. In turn, this allows the same hyphae or hyphal compartment to be monitored over extended periods of time using high-resolution optical microscopy. Furthermore, bacteria can freely move within the system and physical interactions between bacteria and hyphae can be studied with high spatial and temporal resolution. The second device enables complete exchange of the medium surrounding hyphae in less than 4 minutes, where the amount of compound required for such experiments is low. Thanks to the fast fluidic exchange, we are able to determine the time required for hyphae to respond to a stimulus. To demonstrate the efficacy of our approach, both microfluidic platforms are used to study the interaction of the coprophilous basidiomycete, *Coprinopsis cinerea*, with the soil dwelling bacterium *Bacillus subtilis*. *C. cinerea* hyphae secrete antibacterial peptides that are active against Gram-positive bacteria such as *B. subtilis*,[33] whilst *B. subtilis* exhibits antifungal activity,[34] providing an interesting BFI. Our new analytical technology provides novel and surprising insights into the fungal lifestyle and the "mode of action" of BFIs at a cellular level.

Results and discussion

Device structure

The two devices detailed herein were fabricated using a structured PDMS top layer, containing micron-sized features, and a glass-bottomed petri dish as the bottom layer. Upon sealing the two layers together, following oxygen plasma treatment, microchannels were filled immediately with the medium of choice. *C. cinerea* was grown on yeast–malt extract–glucose (YMG) agar for three days at 28 °C and a fungal inoculum, taken from the peripheral growth zone, was placed next to the opening of the microchannels, as illustrated in Fig. 1a. The entire device was incubated in a dark, humid environment for 18 hours, under constant temperature (28 °C), during which time hyphae grow and enter the microchannels. An agar plug containing the fungal mycelium was used to introduce hyphae into the device; however, it is important to note that the device design can easily be adapted to allow incorporation and germination of individual fungal spores.

The first device design, which we term the BFI device, is detailed in Fig. 1 and provides an environment whereby bacteria can interact with hyphae of *C. cinerea*. Device operation is detailed fully in Method 1 (ESI†). The key components of this device include (i) 28 microchannels arranged in parallel, where hyphae are confined in the *z*-direction, (ii) a constriction point, which limits and controls the number of hyphae entering each microchannel, and (iii) an inlet, where bacteria are introduced into the system. Each hyphal observation channel is 110 μm in

Downloaded from https://academic.oup.com/ib/article-abstract/6/10/935/5199045 by ETH Zürich user on 21 February 2019

 This journal is © The Royal Society of Chemistry 2014

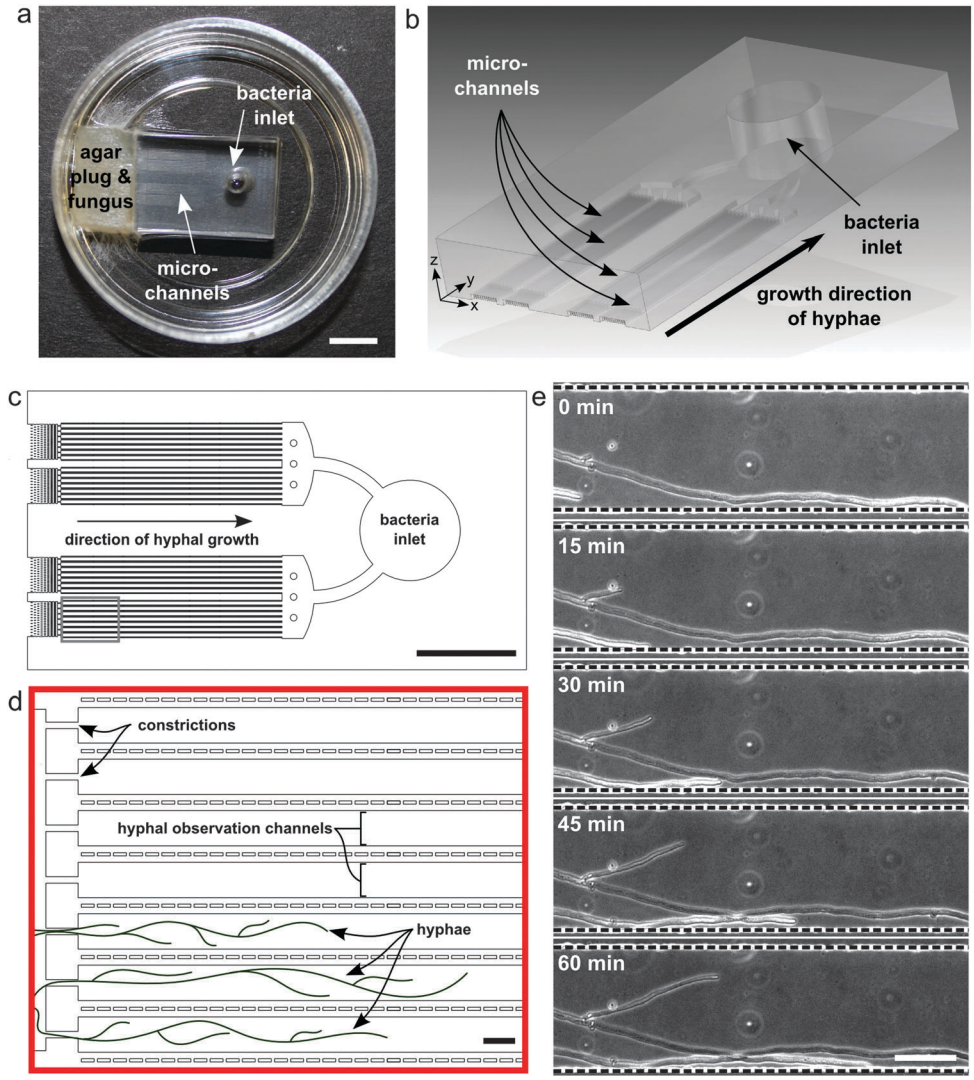

Fig. 1 Design and operation of the BFI device. (a) Photograph illustrating the experimental setup. A PDMS top layer, containing microchannels embossed into its surface, is bonded to a glass petri dish and the channels filled with aqueous medium. A fungal inoculum is placed next to the opening of the microchannels. Following incubation, the device can be co-inoculated with bacteria at the 'bacterial inlet'. Scale bar, 5 mm. (b) Three-dimensional representation of the PDMS top layer containing the microchannels. The entrance to the microchannels can be observed and the growth direction of the hyphae is highlighted. (c) Two-dimensional representation of the BFI device illustrating its key features: constrictions for limiting the number of hyphae entering into the device and hyphal observation channels for monitoring bacterial–fungal interactions for up to 24 h. Scale bar, 3 mm. (d) Enlarged region of the design, depicted by the red box. Scale bar, 100 μm. (e) An example of *C. cinerea* hyphae growing in the microchannels. A branching event and clamp cell formation can be observed (see ESI,† Movie 1). Scale bar, 50 μm.

width, nearly 7 mm in length and 10 μm in depth, with a constriction width of 20 μm. A channel depth of 10 μm was chosen, primarily to confine *C. cinerea* hyphae (which have a diameter of approximately 7 μm) but also to provide sufficient room for bacteria to interact with the hyphae. A channel width of 110 μm provides more space for hyphal extension, enabling branching events and bacterial associations to be visualised. The bacterium, *B. subtilis*, has a length on the order of 1 μm and can therefore navigate around the hyphae within a microchannel. The long, narrow microchannels permit long-term time-lapse imaging to be conducted, allowing hyphal growth to be monitored for up to 24 h. Fig. 1e shows a leading hypha growing in a microchannel at an average rate of 4.2 ± 1.0 μm min^{-1}; we determined a branch growth rate (mean ± standard deviation) of 2.1 ± 0.2 μm min^{-1}. Further, clamp cell and septa formation were observed (see ESI,† Movies 1 and 2). As the microchannel dimensions act to confine the length of a single hypha, as well as subsequent branching events, the volume directly surrounding each hypha is limited. Hence, an environment whereby bacteria can be confined in the vicinity of each hypha is afforded and dynamic interactions between bacteria and hyphae may be monitored. To introduce bacteria and to allow interaction with hyphae, 10 μL of a bacterial suspension (containing bacteria in *C. cinerea* minimal medium (CCMM) with an optical density at 600 nm of 1) was pipetted into the device inlet. As *B. subtilis* is a motile bacterium, it is able to explore its environment and interact with the fungal hyphae independently, as illustrated in Movie 3 (ESI†). Moreover, as this is a closed system, the spatial

Downloaded from https://academic.oup.com/ib/article-abstract/6/10/935/5199045 by ETH Zürich user on 21 February 2019

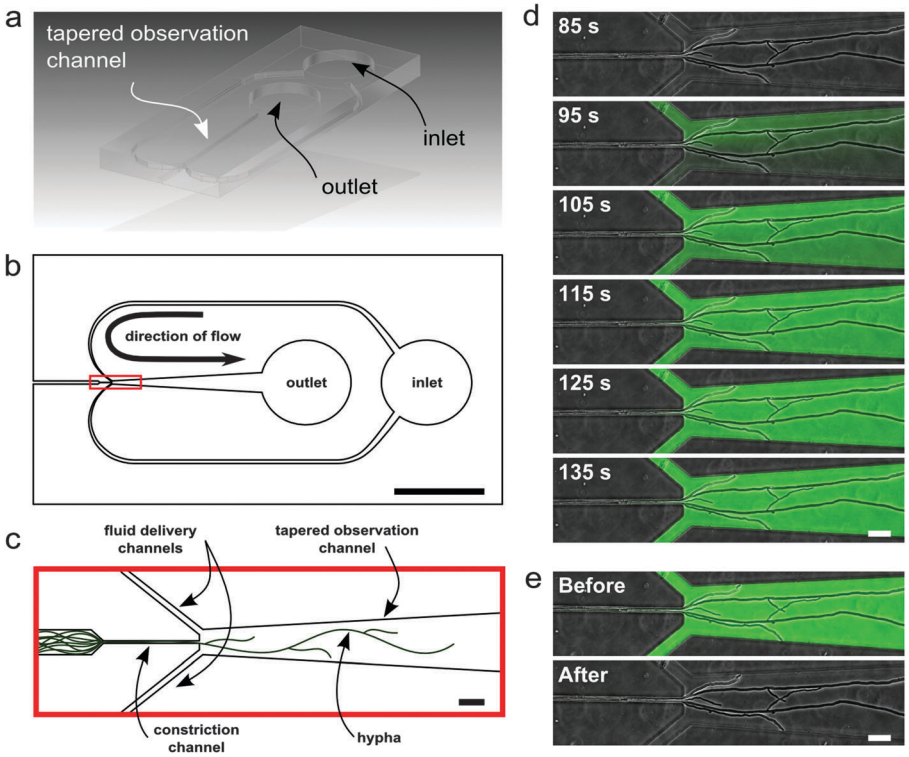

Fig. 2 Design and operation of the fluid exchange device. (a) Three-dimensional and (b) two-dimensional representations of the fluid exchange device highlighting its key features. Scale bar, 3 mm. (c) An enlarged region of the design, specifically depicted by the red box in (b). A tapered observation channel and a narrow constriction channel were used to manipulate the direction of fluid flow towards the outlet, providing regions of low and high resistance respectively. Fluid delivery channels were located at the entrance of the tapered observation channel to minimise blockages by growing hyphae. Scale bar, 100 μm. (d) Time-lapse of CCMM exchange with a fluorescein solution using the fluid exchange device (brightfield and fluorescence channels merged). Full (100%) exchange took place within 3–4 minutes (see ESI,† Fig. S1 and S2 for control experiments). Scale bar, 50 μm. (e) Before and after removal of the fluorescein solution with CCMM. Scale bar, 50 μm.

distribution of the bacteria relative to the hyphae and their dynamic interactions could be monitored in real time, without dilution. The advantages of this device are that bacteria are free to explore their environment, interacting with hyphae, and several channels can be monitored at the same time, serving as "technical" repeats for the experiment.

The ability to access and manipulate the fluid surrounding the hyphae is a desirable function. As this cannot be achieved in a direct way using the BFI device, a second device was designed for this specific purpose and is termed the fluid exchange device. Fig. 2a–c illustrate a three-dimensional representation of the device design and the mask design respectively (operation is described in Method 1 (ESI†)).

The fluid exchange device acts to passively pump fluid into the main observation channel and possesses a constriction channel, a tapered observation channel, an inlet and an outlet. The constriction channel was designed to be 10 μm in both width and height, with a length of 400 μm, thus limiting the number of hyphae entering the observation channel. More importantly, the hyphae are exploited as a means to block the constriction junction, providing a region of high fluidic resistance, which diverts the flow to the outlet *via* a tapered observation channel. This channel creates a zone of lower fluidic resistance in the direction of the outlet. As such, there is minimal interaction of the substance of interest with the rest of the mycelium. It was found that the ideal location of the delivery channels (which transfer material from the inlet to the main observation channel) is situated at the beginning of the tapered observation channel. When a hypha first passes through the constriction channel and enters the tapered channel, it grows in a polarised manner towards the outlet. Hyphal tips are often observed tracking the edge of the microchannel (see ESI,† Movie 4) and branching events occur at angles between 70 and 75 degrees[35] relative to the main hyphal body (in the direction of the tip). Accordingly, the placement of the delivery channels at the beginning of the tapered observation channel opposes the natural polarised growth of hyphae, minimizing any blockage of channels due to fungal growth.

To demonstrate operation, CCMM was exchanged with an aqueous, fluorescein-containing solution. It was found that fluid exchange occurs in less than 4 minutes (Fig. 2d and ESI,† Fig. S1) and 100% exchange of the fluid was achieved when washing steps were incorporated into the exchange process (see ESI,† Method 2 and Fig. S2). Fig. 2e illustrates complete removal of a fluorescein solution from the main observation channel, when exchanged with CCMM. Importantly, control experiments, where CCMM was exchanged with CCMM, do not result in an arrest of hyphal growth. To summarise, the

Downloaded from https://academic.oup.com/ib/article-abstract/6/10/935/5199045 by ETH Zürich user on 21 February 2019

 This journal is © The Royal Society of Chemistry 2014

advantages associated with the fluid exchange device include the ability to exchange or collect media directly surrounding hyphae and the ability to introduce both, motile and non-motile, bacteria accordingly. The fluid exchange device opens up new avenues, where hyphae can be interrogated with specific biochemical agents and the response monitored in real time. In addition, live/dead assays can be conducted and the chemical and biological species expressed by the fungus in the presence of different bacteria (and *vice versa*) can be analysed directly.

Interaction between *C. cinerea* and *B. subtilis* in the BFI device

We applied the microfluidic device to monitor the interaction of *C. cinerea* with *B. subtilis*. Different *Bacillus* species produce biologically active lipopeptides from the surfactin, iturin and fengycin families,[34] with many of these lipopeptides showing antifungal properties. The confrontation of *C. cinerea* strain AmutBmut with two different strains of *B. subtilis*, the laboratory strain, *B. subtilis* 168, and the wild-strain, *B. subtilis* NCIB 3610,[36] was initially performed on a CCMM agar plate as a classical confrontation assay (Fig. 3a). Growth inhibition of *C. cinerea* was observed only in the presence of *B. subtilis* NCIB 3610, as indicated by clear exclusion zones. Previous studies have demonstrated that this *B. subtilis* strain produces antifungal agents that inhibit the growth of different plant pathogenic oomycetes and ascomycetes,[37] whereas the laboratory strain, *B. subtilis* 168, does not produce any of the antifungal lipopeptides.[38] The confrontation assay defined the growth inhibitory action of *B. subtilis* NCIB 3610 at a macroscopic level and without direct contact, but revealed little information regarding the mode of interaction between the two organisms. Accordingly, we used the BFI device to monitor the physical interaction of bacteria with hyphae over time. Upon addition of the two *B. subtilis* strains into the microfluidic system, attachment of bacteria to the hyphae in an end-on manner was observed (Fig. 3b and c), suggesting that the bacterial binding site was exposed at the bacterial cell pole. To visualise the attachment pattern, *C. cinerea* strain AmutBmut pMA412, expressing the cytoplasmic fluorescent dTomato protein under the control of the constitutive *Agaricus bisporus gpd*II promoter,[39] and *B. subtilis* pMF37, expressing the green fluorescent protein (gfp) under the control of the constitutive hyper *spac* promoter integrated into the *amyE* locus,[40] were introduced into the BFI device. Interestingly, bacteria attached only to certain hyphae (Fig. 4) and no attachment to the newly formed surface of growing hyphae was detected: the zone extending from the growing hyphal tip was free of attaching bacteria. In this apical growing organism the cell wall is assembled at the tip and undergoes a subsequent maturation process.[41] This suggests that the structure where bacteria attach to on hyphae is not yet present on these newly formed surfaces. Furthermore, bacterial attachment was observed on some branches but not on their corresponding leading hyphae (see ESI,† Fig. S3). These branches were competent for attachment and hence differentiated from their leading hyphae. Septa of higher fungi can be opened and closed and therefore cells within hyphae can serve as differentiated entities.[42,43] This attachment pattern was identical for both bacterial strains, suggesting that some hyphae were competent for bacterial attachment while others were not. However, the binding site on the competent hyphae is unknown. Bacteria killed using ultraviolet illuminations (see ESI,† Method 3) and introduced subsequently to *C. cinerea* hyphae also attached to the hyphae in the same way. We concluded that hyphal differentiation and competence for attachment was present prior to hyphae and

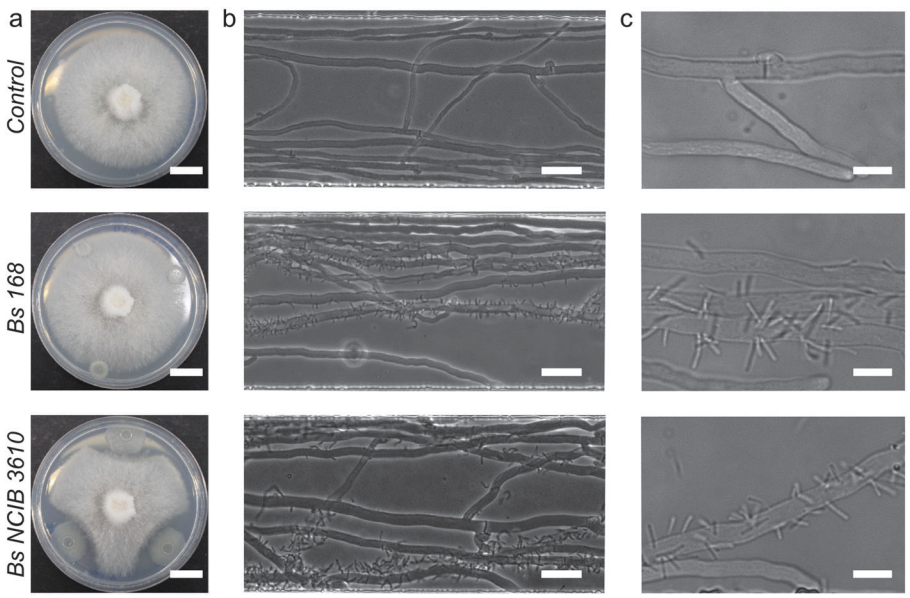

Fig. 3 Interaction of *C. cinerea* with two different *B. subtilis* strains. (a) Confrontation assay on CCMM agar plates illustrating the different response of *C. cinerea* growth alone (top) and in the presence of *B. subtilis* 168 (*Bs* 168, middle) and *B. subtilis* NCIB 3610 (*Bs* NCIB 3610, bottom). A growth inhibition zone was observed only upon co-inoculation with *B. subtilis* NCIB 3610. Scale bar, 20 mm. Panels (b) and (c) represent exemplar data that were gained at the microlevel using the BFI device. The physical interaction between *C. cinerea* hyphae and *B. subtilis* cells was observed. The polar attachment of bacteria to the hyphae and attachment of bacteria to certain hyphae was the same for both *B. subtilis* strains. Scale bars in (b) and (c), 25 and 10 μm respectively.

Downloaded from https://academic.oup.com/ib/article-abstract/6/10/935/5199045 by ETH Zürich user on 21 February 2019

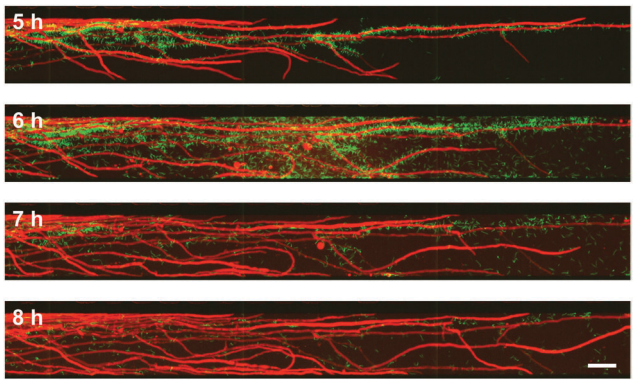

Fig. 4 Attachment pattern of *B. subtilis* to *C. cinerea* hyphae. *B. subtilis* NCIB 3610 pMF37, expressing gfp constitutively, and *C. cinerea* pMA412, expressing dTomato constitutively, were co-inoculated into the BFI device and attachment was monitored over time. Scale bar, 50 μm.

bacteria coming into contact. Our results provided direct evidence for functional differentiation of living hyphae within the mycelium. This differentiation has also been proposed recently by Wösten and co-workers, where differential transcriptional and translational activity[44] and RNA composition in an *Aspergillus niger* mycelium were reported.[45] Differential attachment has also been described for the interaction between *Pseudomonas aeruginosa* and *Candida albicans* hyphae, but only for single hyphae and not within the same mycelium.[46] Toljander *et al.* showed that bacterial attachment differed for living and dead hyphae.[47]

Furthermore, bacterial attachment to hyphae and the local concentration of free bacteria were found to change over time, as illustrated in Fig. 4. Bacterial attachment to hyphae decreased after a high local concentration of free bacteria resided in the vicinity (see Fig. 4). Movies 5 and 6 (ESI†) demonstrate regions containing a high local concentration of *B. subtilis* NCIB 3610 in close proximity to hyphae. Interestingly, these bacterial associations moved along the microchannels in clusters, suggesting a coordinated behaviour of the bacteria. Attachment of bacteria to hyphal cells has been described before[46–50] with some bacteria initially attaching in an end-on manner to the hyphae.[51,52] However, the dynamics of the attachment could not be determined with the methods previously used. Using our BFI device it was observed that the attachment and local bacterial concentration change over time.

We used the same experimental platform to study the long-term growth characteristics of *C. cinerea* leading hyphae in the presence and absence of the two *B. subtilis* strains. *C. cinerea* hyphae were allowed to grow into the BFI device until they reached the observation channels thereby plugging the constriction. Such plugging did not prevent fungal growth in the observation channel. Subsequently, bacteria were introduced into the microchannels *via* the inlet and a time-lapse experiment (30-minute time interval) over the whole length of seven microchannels was conducted. Using the same setup, a control experiment was performed in the absence of bacteria. Fig. 5a shows the change in the growth rate of the leading hyphae with time for each of the aforementioned conditions. The aggregated average growth rate of the leading hyphae in the control experiment was 6.2 ± 1.4 μm min^{-1}, 5.0 ± 1.5 μm min^{-1} in the presence of the laboratory strain, *B. subtilis* 168, and

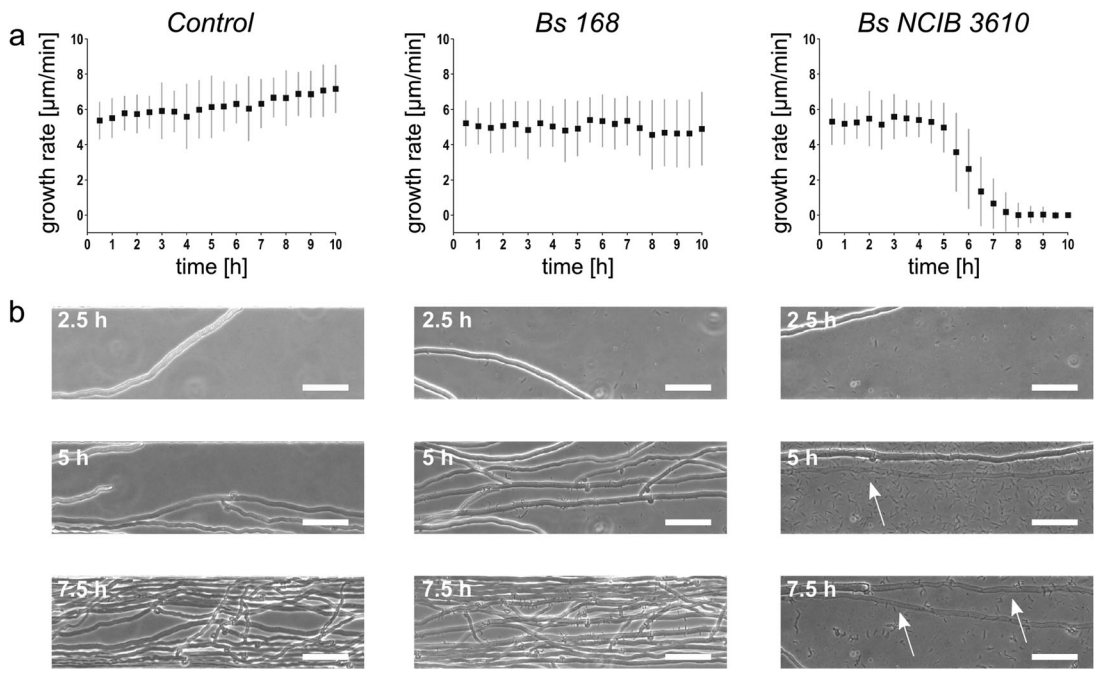

Fig. 5 Long-term observation of *C. cinerea* hyphal growth in the absence and presence of the two *B. subtilis* strains. (a) The growth rate of the leading hyphae was measured in the BFI device over a 10 hour time period in three independent experiments. Error bars represent standard deviations from three independent experiments. The *B. subtilis* NCIB 3610 strain had a negative effect on the growth rate of the leading hyphae that was apparent 5 hours after co-inoculation. (b) Bright field images representing three different time points at the same site for each condition tested. Upon addition of *B. subtilis* NCIB 3610, some hyphae showed a thin morphology (depicted by arrows), whereas this was not observed after the addition of *B. subtilis* 168. Scale bars, 25 μm.

Downloaded from https://academic.oup.com/ib/article-abstract/6/10/935/5199045 by ETH Zürich user on 21 February 2019

 This journal is © The Royal Society of Chemistry 2014

3.1 ± 2.7 μm min^{-1} in the presence of the wild strain, *B. subtilis* NCIB 3610 (mean ± standard deviation). The aggregated average growth rates of the leading hyphae in the presence of *B. subtilis* 168 and *B. subtilis* NCIB 3610 were found to be significantly different from the aggregated average growth rate of the control, with *p*-values of 0.0161 and <0.001 respectively. There was also a significant difference between the aggregated average growth rates of the leading hyphae in the presence of *B. subtilis* 168 and *B. subtilis* NCIB 3610 with a *p*-value of <0.001 (see ESI,† Fig. S4). Upon introduction of the wild-strain, *B. subtilis* NCIB 3610, into the BFI device, it was apparent that the leading hyphae stopped growing (Fig. 5a) after five hours. Additionally, a change in the morphology of some fungal apical cells was observed, which became transparent and thinner in nature (Fig. 5b, arrows). A clear difference in morphology between affected hyphal cells and adjacent cells was observed. Interestingly, branches growing from hyphal cells distal to affected cells continued to propagate, indicating the functionality of the adjoining cells. Importantly, the morphological changes described were not observed for the experiments involving *B. subtilis* strain 168.

To visualise the cellular response of hyphae interacting with *B. subtilis* more precisely, the fluorescent *C. cinerea* strain AmutBmut pMA412 was introduced into the BFI device and co-inoculated with bacteria using the same experimental approach as described above. Fig. 6a details a series of images taken over a period of 8 hours and 20 minutes and illustrates the morphological change that was described above of several cells. These cells resemble collapsed hyphal compartments, with a loss of dTomato fluorescence. Simultaneously, we observed blebs containing fluorescent dTomato emerging from these hyphal compartments (Fig. 6a and b and ESI,† Movie 7), most likely the cause for the loss of cellular content in these cells. Some of the blebs were stable for up to several hours. The confined location of extracellular dTomato fluorescence suggests that these blebs consisted of membranes encompassing the cytoplasmic content. This process takes place mainly in apical cells and, interestingly, did not show any correlation with the attachment of bacteria to the hyphae. Fig. 6b exemplifies a collapsed hyphal compartment: two adjoining cells were still intact five hours after the addition of the *B. subtilis* wild-strain; however, one of these hyphal compartments had collapsed within the next 30 minutes. The distal cell remained intact, indicating that the dolipore was closed. These experiments demonstrated that *B. subtilis* NCIB 3610 was capable of arresting

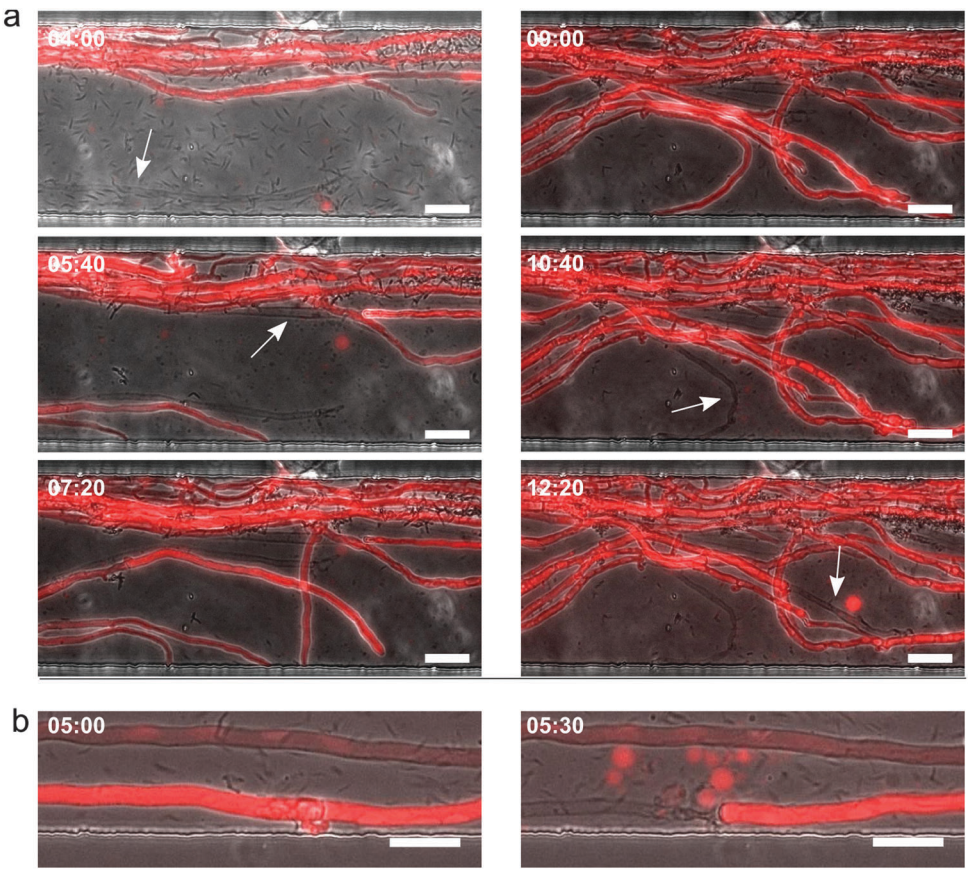

Fig. 6 Morphological changes of *C. cinerea* hyphae in the presence of *B. subtilis*. (a) A co-inoculation time-lapse experiment was conducted with a *C. cinerea* strain that expresses dTomato under the control of a constitutive promoter using the BFI device. The arrows highlight cells that have lost their cellular contents due to the presence of *B. subtilis* NCIB 3610. Timestamps indicate the time after inoculation of the device with bacteria. Scale bar, 25 μm. See also ESI,† Movie 7. (b) Depiction of a hypha that was intact at the 5 hour time point. One cell collapsed within the next 30 min. Blebs containing cellular content were located next to this hyphal cell. Scale bar, 25 μm. Time format, hh:mm.

Downloaded from https://academic.oup.com/ib/article-abstract/6/10/935/5199045 by ETH Zürich user on 21 February 2019

growth of the leading hyphae by inducing collapse of some of the hyphal compartments. Interestingly, bacterial attachment did not correlate with the collapse of hyphal compartments. Contrarily, attachment of *P. aeruginosa* to *C. albicans* hyphae leads to the establishment of biofilms and is important for the subsequent contact mediated killing of hyphae.[46,52]

Effect of *B. subtilis* cell-free supernatant on *C. cinerea* hyphae

To elucidate if the direct interaction of bacteria with hyphae was required for the fungicidal effect observed, *B. subtilis* cell-free supernatant (see ESI,† Method 4) was tested on *C. cinerea* pMA412 hyphae. The two *B. subtilis* strains were sub-cultured in CCMM for 20 hours in the absence of *C. cinerea*. Bacteria were removed by centrifugation and the sterile-filtered supernatant was added to *C. cinerea* hyphae using the fluid exchange device. After exchange of CCMM with the *B. subtilis* NCIB 3610 conditioned medium, hyphal apical cells collapsed in a fashion comparable to that observed in the presence of bacteria – that is, with the occurrence of blebs (Fig. 7a and b and ESI,† Movie 8). Moreover, it was apparent that the shape of the hyphal tip changed first, a few minutes after application of the conditioned medium. Blebbing was observed only for some apical cells, but all hyphae stopped growing after the addition of the conditioned medium from *B. subtilis* NCIB 3610. As expected, this did not occur when the medium surrounding the hyphae was exchanged with *B. subtilis* 168 conditioned medium (ESI,† Fig. S5).

It is well known that some *Bacillus* lipopeptides harbour antifungal effects, especially lipopeptides from the iturin and fengycin families which are active against filamentous fungi.[13,14,53–56] Both *B. subtilis* strains contain non-ribosomal peptide synthase (NRPS) gene clusters to produce the lipopeptides surfactin and fengycin. Due to a mutation in *sfp*, whose gene product is required for the activation of both NRPSs, *B. subtilis* 168 does not produce these lipopeptides.[57,58] Therefore, we assessed whether lipopeptides were responsible for the blebbing phenotype. Taking advantage of the fact that lipopeptides are *n*-butanol extractable and thermostable,[14,53] we extracted components from conditioned medium with *n*-butanol, evaporated it to dryness and resuspended the dried film in CCMM. The morphological changes of *C. cinerea* hyphae, upon addition of this solution, were monitored in the exchanging device. Additionally, we heat treated the conditioned medium for 15 min at 100 °C. Both treatments did not abolish the formation of blebs nor the collapse of apical cells (see ESI,† Table S1). To exclude any effect due to the remaining *n*-butanol, the medium was exchanged with CCMM containing 1% (v/v) *n*-butanol. No growth stop or collapse of apical cells was observed. These experiments suggest that growth arrest and the formation of blebs were both elucidated by *n*-butanol extractable activities and not by enzymes produced by the bacteria. Importantly, this activity affected cell wall properties and not plasma membrane permeability, because cytoplasm-containing blebs were observed. A similar observation was also reported for the *Bacillus amyloliquefaciens* action on *Fusarium oxysporum* hyphae.[59] These experiments also demonstrate different modes of experimentation that become possible using the fluid exchange device.

Experimental

Strains and cultivation conditions

Fungal and bacterial strains used in this study are summarised in Table S2 (ESI†). *Escherichia coli* DH5α was used for cloning and maintenance of plasmids. Preparation of transformation competent cells was carried out as described by Inoue *et al.*[60] *E. coli* DH5α containing pMF37 and pRS426 plasmids and their derivatives was selected on Luria–Bertani (LB) medium containing 100 μg mL^{-1} ampicillin (see ESI†). *Saccharomyces cerevisiae* laboratory strain W303a (*MAT*a *ade2-1 leu2-3,112 his3 ura3-1 can1-100 trp1-1*) was used for homologous recombination of plasmids and was maintained on yeast extract–peptone–dextrose (YPD) medium (see ESI†) at 30 °C and transformants were selected on synthetic complete dextrose without uracil (SD Ura−) agar plates.[61] The laboratory strain, *B. subtilis* 168, and the wild-strain, *B. subtilis* NCIB 3610, were maintained on LB medium, and the *B. subtilis* strains containing inserted pMF37 plasmids were maintained on LB medium with 100 μg mL^{-1} spectinomycin. *E. coli* and

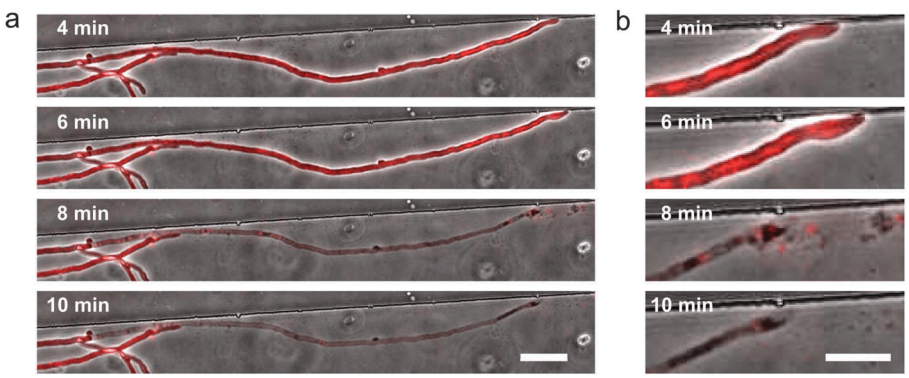

Fig. 7 Effect of bacteria-cell free conditioned medium on *C. cinerea* hyphae. (a) Addition of cell-free conditioned medium from *B. subtilis* NCIB 3610 to *C. cinerea* hyphae expressing dTomato constitutively. After exchange of CCMM with the conditioned medium the form of the tip changed within a few minutes. This was followed by formation of blebs after eight minutes (see ESI,† Movie 8). Scale bar, 50 μm. (b) Enlarged view of the tip depicted in (a). After eight minutes the formation of blebs occurred. Scale bar, 25 μm. (c) Uniform growth of *C. cinerea* hyphae in the exchange device is depicted before the addition of surfactin in the first column. Scale bar, 100 μm. Brightfield and fluorescence channels merged for all images.

Downloaded from https://academic.oup.com/ib/article-abstract/6/10/935/5199045 by ETH Zürich user on 21 February 2019

 This journal is © The Royal Society of Chemistry 2014

B. subtilis strains were grown aerobically at 37 °C if not otherwise stated. *C. cinerea* strain AmutBmut[62] was cultivated on solid YMG medium (see ESI†) at 28 °C in a dark and humid environment.

Plasmids

Plasmids and primers used in this study are listed in Tables S3 and S4 (ESI†), respectively. Cloning by homologous recombination was carried out in *S. cerevisiae* W303a as described previously.[61] Construction of plasmid pMA412 is described in Method 5 (ESI†). Plasmids were transformed into *C. cinerea* strain AmutBmut by protoplasting of the mononucleate asexual spores (oidia) as described previously.[63] Plasmid pMF37 was integrated into the *amyE* locus on the chromosome by homologous recombination. The plasmid was introduced into *B. subtilis* cells by natural competence.[64]

Confrontation assay on agar plates

An agar plug with *C. cinerea* grown on YMG medium was inoculated in the centre of a CCMM (see ESI†) agar plate. Bacteria, taken from an overnight culture, were diluted with LB using a 1 : 25 ratio and sub-cultured aerobically for 3 h at 37 °C. Bacteria were washed once with a 0.9% w/v sodium chloride solution and resuspended in CCMM to an optical density at 600 nm (OD_{600}) of 2. Three times 5 μL aliquots of the bacterial suspension were placed equidistant (3.5 cm) from the centre of the agar plate. The plates were incubated for 5 days at 28 °C in a humid and dark environment.

Device preparation

Devices were designed in AutoCAD Mechanical 2011 (Autodesk) and used to create mylar film photolithography masks (Micro Lithography Services Ltd., UK). Each master mold was manufactured using conventional photolithography techniques[65] (see ESI,† Method 6 for full details). Before use with PDMS, the masters were silanised under vacuum for 2 hours with 50 μL chlorotrimethylsilane (Fluka, Germany) per master.

50 g of PDMS was prepared (per master) using a 10 : 1 ratio of base to curing agent (Sylgard 184, Dow Corning, USA). The base and the curing agent were mixed together thoroughly, degassed for 1 hour under vacuum and poured on top of the master. This mixture was then cured in an oven at 70 °C for >2 hours. The cured PDMS was removed from the master and diced to size. Holes were punched into the PDMS at specific locations, using a 3.02 mm diameter precision cutter (Syneo, USA), to form the channel inlets and outlets.

Each PDMS slab was then bonded to a glass-bottomed Petri dish (dish diameter: 35 mm; glass diameter: 23 mm; glass thickness: 0.17 mm; World Precision Instruments, Inc., Germany) to close the microchannels. First, the PDMS slabs (after removal of scotch tape) and Petri dishes were washed and dried (see ESI,† Method 7). Bonding of PDMS to the glass-bottomed Petri dishes was achieved by activating the surfaces using a glow discharge unit (EMITECH K1000X, Quorum Technologies, UK) under the following conditions: polarity, negative; cycle vacuum point, 1×10^{-1} mbar; plasma current, 25 mA; coating time, 1 min. Proceeding activation, the hydrophilic surfaces were brought into conformal contact with one another to form a bond and 100 μL of CCMM was used to fill the microchannels of each device (*via* capillary action). An additional 100 μL of CCMM was introduced into the glass-bottomed Petri dish to maintain a humid environment upon closing the Petri dish. Devices were freshly prepared for each experiment in a sterile hood and used immediately. Device operation is described in Method 1 (ESI†).

Inoculation of devices with fungus

Prior to inoculation of the microfluidic devices *C. cinerea* was sub-cultured at 28 °C in a dark, aerated, humid box for 3 days. Specifically, a section of the fungal mycelium is cut from the YMG agar plate. A section is taken from the peripheral growth zone and this inoculum is placed next to the device opening, such that the mycelium is in contact with the glass substrate and the growth direction of the hyphal tips is orientated towards the microchannel(s). Care was taken to control the size of the agar plug inoculum to ensure consistency between experiments. The Petri dish was incubated in a dark and humid environment for a period of 18 hours at 28 °C to allow the hyphae to grow into the microchannels.

Live-cell imaging of hyphae

A widefield fluorescence microscope, based on a Nikon Ti-U inverted microscope, was used to acquire long-term time-lapse experiments and was equipped with a Prior ProScan III motorised stage (Prior Scientific, UK) and a CoolSNAP HQ2 camera (Photometrics, Germany). Phase contrast microscopy was performed to capture brightfield images, using either ×10/0.30 NA (numerical aperture) Plan Fluor or ×20/0.45 NA S Plan Fluor objective lenses (Nikon, Switzerland) and an exposure time of 100 ms.

Conventional epifluorescence microscopy was also performed to image hyphae from the *C. cinerea* AmutBmut strain expressing dTomato, the *B. subtilis* strains expressing gfp and the fluorescein-containing solution. A Nikon Intensilight C-HGFI mercury lamp (Nikon, Switzerland) was used as the source of excitation and an exposure time of 100 ms was implemented. The following filter sets were used: TRITC and FITC HC BrightLine Basic Filtersets (AHF Analysentechnik, Germany).

Micromanager (version 1.4.12) was used to coordinate long-term time-lapse imaging experiments. Auto-focus software (Simple Auto Focus, Micromanager) was implemented to correct for drift in the *z*-direction, induced over the long-term, multi-position time-lapse experiments. All long-term time-lapse experiments were performed in a dark room, where the temperature was maintained at 20 °C. The Petri dish was sealed with Parafilm to prevent evaporation and remained in the dark throughout the duration of the time-lapse experiments (other than during image acquisition) to minimise the onset of fungal developmental processes.

Image montages were generated using custom software and analysed using Fiji.[66] To measure the growth difference between the time points and the cell length of the leading hyphae in each microchannel the free hand tool and measuring tool of Fiji were used.

Downloaded from https://academic.oup.com/ib/article-abstract/6/10/935/5199045 by ETH Zürich user on 21 February 2019

Conclusions

Investigations on BFIs using our microfluidic platforms provided several significant advantages. They enabled fungal hyphae to be cultured in microchannels, where hyphae were constricted by the channel height and were thus easily imaged. Such platforms are compatible with high-resolution microscopy techniques (phase contrast, differential interference contrast, confocal, spinning disk confocal) and therefore allow live-cell imaging and long-term, time-lapse microscopy to be conducted with ease. Using the BFI device, we monitored the dynamic interactions of bacteria with hyphae in real-time and with single cell resolution. The presence of several parallel microchannels enabled many growing *C. cinerea* hyphae to be assayed per experiment and their response, upon introduction to bacteria, to be monitored over a period of up to 24 hours (the device architecture can easily be tuned to suit the growth rate of any filamentous fungus of interest). Conversely, the response of bacteria to hyphae was also elucidated. It is anticipated that the coupling of high pressure liquid chromatography, mass spectrometry and automated image processing algorithms with these platforms will increase the functionality of this tool, providing further opportunities to quantify the unique interactions between filamentous fungi and bacteria. We were able to subject hyphae to a variety of stimuli, in a rapid and controlled manner, and to monitor hyphal reaction in real-time using the fluid exchange device.

We took advantage of the simplicity of the fluidic network and introduced the bacteria into the BFI device by simple pipetting. Their interaction with fungal hyphae was monitored in real-time, while the fluid exchange device utilised small differences in hydrostatic pressure to drive the flow and therefore enabled an exchange of the media surrounding hyphae. We note that these microfluidic platforms are simple to integrate within the microbiology laboratory and can be adopted for widespread use.

As a proof of principle we used these platforms to probe the interaction of *C. cinerea* with *B. subtilis*. *B. subtilis* is well known for its antagonising effects on fungi;[34] however our new approach provides novel insights into this interaction at the cellular level and in real-time. We observe that hyphae stop growing with the formation of extracellular, cytoplasm-filled blebs after contact with the wild-strain *B. subtilis* NCIB 3610, but continue to grow in the presence of the laboratory strain *B. subtilis* 168. Growth arrest was induced by a secreted signal because addition of conditioned medium using the fluid exchange device resulted in the same fungal phenotype. Furthermore, both *B. subtilis* strains displayed a direct cellular contact with fungal hyphae that changed over time.

The design and application of microfluidic platforms has allowed us to monitor BFIs at a cellular level and we observed hyphal differentiation of a mycelium and bacteria-induced blebbing of hyphal cells. Studying BFIs using these microfluidic platforms can provide us with an understanding of how micro-organisms use their antagonistic strategies in competing environments, as well as allow the production of antimicrobial substances in time and space to be located and quantified. Moreover, the technique enables the study of dynamic processes, such as quorum sensing of bacterial cells in BFIs, using promoter–reporter fusions. In combination with genetic and biochemical tools, microfluidic platforms provide an optimal experimental set-up to characterise the interaction of fungi with bacteria at a cellular level.

Further, it is envisaged that this technology will not only impact research involving BFIs, but will also serve as a means to study other fungal antagonists and mutualists such as nematodes, plants and other fungi.

Acknowledgements

The authors would like to thank C. Villalba for construction of plasmid pMK317, Prof. Uwe Sauer, Prof. Richard Losick, Prof. Masaya Fujita and Dr Daniel Lopez for providing *B. subtilis* strains and plasmids, Oliver Dressler and Adam Sheldon for custom software design, Patrick Stöckli for 3-D illustrations, Dr Stavros Stavrakis for discussions concerning microscopy and Matteo Tanadini for help with statistical analysis. This work was supported by ETH Research Grant ETH-34 11-2 and EMBO Grant ASTF 317-2010.

References

1 P. Frey-Klett, P. Burlinson, A. Deveau, M. Barret, M. Tarkka and A. Sarniguet, *Microbiol. Mol. Biol. Rev.*, 2011, **75**, 583–609.
2 F. Zarenejad, B. Yakhchali and I. Rasooli, *World J. Microbiol. Biotechnol.*, 2012, **28**, 99–104.
3 A. Deveau, B. Palin, C. Delaruelle, M. Peter, A. Kohler, J. C. Pierrat, A. Sarniguet, J. Garbaye, F. Martin and P. Frey-Klett, *New Phytol.*, 2007, **175**, 743–755.
4 W. de Boer, L. Folman, R. Summerbell and L. Boddy, *FEMS Microbiol. Rev.*, 2005, **29**, 795–811.
5 A. Peleg, D. Hogan and E. Mylonakis, *Nat. Rev. Microbiol.*, 2010, **8**, 340–349.
6 B. Mogge, C. Loferer, R. Agerer, P. Hutzler and A. Hartmann, *Mycorrhiza*, 2000, **9**, 271–278.
7 G. F. Bills, J. B. Gloer and Z. An, *Curr. Opin. Microbiol.*, 2013, **16**, 549–565.
8 J. Moller, M. B. Miller and A. Kjoller, *Soil Biol. Biochem.*, 1999, **31**, 367–374.
9 A. A. Brakhage, *Nat. Rev. Microbiol.*, 2013, **11**, 21–32.
10 T. Schneider, T. Kruse, R. Wimmer, I. Wiedemann, V. Sass, U. Pag, A. Jansen, A. K. Nielsen, P. H. Mygind, D. S. Raventós, S. Neve, B. Ravn, A. M. Bonvin, L. De Maria, A. S. Andersen, L. K. Gammelgaard, H. G. Sahl and H. H. Kristensen, *Science*, 2013, **328**, 1168–1172.
11 H. Nützmann, Y. Reyes-Dominguez, K. Scherlach, V. Schroeckh, F. Horn, A. Gacek, J. Schümann, C. Hertweck, J. Strauss and A. Brakhage, *Proc. Natl. Acad. Sci. U. S. A.*, 2011, **108**, 14282–14287.
12 C. R. Howell and R. D. Stipanovic, *Phytopathology*, 1979, **69**, 480–482.
13 Y. Touré, M. Ongena, P. Jacques, A. Guiro and P. Thonart, *J. Appl. Microbiol.*, 2004, **96**, 1151–1160.

Downloaded from https://academic.oup.com/ib/article-abstract/6/10/935/5199045 by ETH Zürich user on 21 February 2019

 This journal is © The Royal Society of Chemistry 2014

14 D. Romero, A. De Vicente, R. H. Rakotoaly, S. E. Dufour, J. W. Veening, E. Arrebola, F. M. Cazorla, O. P. Kuipers, M. Paquot and A. Perez-Garcia, *Mol. Plant-Microbe Interact.*, 2007, **20**, 430–440.
15 C. Calderón, A. de Vicente and F. Cazorla, *FEMS Microbiol. Ecol.*, 2014, **89**, 20–31.
16 G. I. Souto, O. S. Correa, M. S. Montecchia, N. L. Kerber, M. Bachur and A. F. Garcia, *J. Appl. Microbiol.*, 2004, **97**, 1247–1256.
17 G. Wichmann, J. Sun, K. Dementhon, N. L. Glass and S. E. Lindow, *Mol. Microbiol.*, 2008, **68**, 672–689.
18 A. J. deMello, *Nature*, 2006, **442**, 394–402.
19 F. Pereira, X. Niu and A. J. deMello, *PLoS One*, 2013, **8**, e63087.
20 A. Fallah-Araghi, J. C. Baret, M. Ryckelynck and A. D. Griffiths, *Lab Chip*, 2012, **12**, 882–891.
21 T. Ahmed, T. S. Shimizu and R. Stocker, *Nano Lett.*, 2010, **10**, 3379–3385.
22 D. B. Weibel, W. R. DiLuzio and G. M. Whitesides, *Nat. Rev. Microbiol.*, 2007, **5**, 209–218.
23 J. N. Lee, X. Jiang, D. Ryan and G. M. Whitesides, *Langmuir*, 2004, **20**, 11684–11691.
24 J. C. McDonald and G. M. Whitesides, *Acc. Chem. Res.*, 2002, **35**, 491–499.
25 A. K. Wessel, L. Hmelo, M. R. Parsek and M. Whiteley, *Nat. Rev. Microbiol.*, 2013, **11**, 337–348.
26 S. Park, P. M. Wolanin, E. A. Yuzbashyan, H. Lin, N. C. Darnton, J. B. Stock, P. Silberzan and R. Austin, *Proc. Natl. Acad. Sci. U. S. A.*, 2003, **100**, 13910–13915.
27 D. Koley, M. M. Ramsey, A. J. Bard and M. Whiteley, *Proc. Natl. Acad. Sci. U. S. A.*, 2011, **108**, 19996–20001.
28 H. Mao, P. S. Cremer and M. D. Manson, *Proc. Natl. Acad. Sci. U. S. A.*, 2003, **100**, 5449–5454.
29 J. Q. Boedicker, M. E. Vincent and R. F. Ismagilov, *Angew. Chem., Int. Ed.*, 2009, **48**, 5908–5911.
30 E. C. Carnes, D. M. Lopez, N. P. Donegan, A. Cheung, H. Gresham, G. S. Timmins and C. J. Brinker, *Nat. Chem. Biol.*, 2010, **6**, 41–45.
31 M. Held, C. Edwards and D. V. Nicolau, *Fungal Biol.*, 2011, **115**, 493–505.
32 J. Park, A. Kerner, M. A. Burns and X. Nina Lin, *PLoS One*, 2011, **6**, e17019.
33 A. Essig, D. Hofmann, D. Münch, S. Gayathri, M. Kuenzler, P. T. Kallio, H.-G. Sahl, G. Wider, T. Schneider and M. Aebi, 2014, unpublished.
34 K. Nagorska, M. Bikowski and M. Obuchowski, *Acta Biochim. Pol.*, 2007, **54**, 495–508.
35 U. Kües, *Microbiol. Mol. Biol. Rev.*, 2000, **64**, 316–353.
36 D. R. Zeigler, Z. Prágai, S. Rodriguez, B. Chevreux, A. Muffler, T. Albert, R. Bai, M. Wyss and J. B. Perkins, *J. Bacteriol.*, 2008, **190**, 6983–6995.
37 Y. Chen, F. Yan, Y. Chai, H. Liu, R. Kolter, R. Losick and J. H. Guo, *Environ. Microbiol.*, 2012, **15**, 848–864.
38 V. Leclère, R. Marti, M. Béchet, P. Fickers and P. Jacques, *Arch. Microbiol.*, 2006, **186**, 475–483.
39 C. Burns, K. E. Gregory, M. Kirby, M. K. Cheung, M. Riquelme, T. J. Elliott, M. P. Challen, A. Bailey and G. D. Foster, *Fungal Genet. Biol.*, 2005, **42**, 191–199.
40 M. Fujita and R. Losick, *Mol. Microbiol.*, 2002, **43**, 27–38.
41 J. G. H. Wessels, in *Role of Cell Wall Architecture in Fungal Tip Growth Generation*, ed. I. B. Heath, Academic Press, New York, 1990, ch. 1, pp. 1–29.
42 R.-J. Bleichrodt, G. J. van Veluw, B. Recter, J.-I. Maruyama, K. Kitamoto and H. A. B. Wösten, *Mol. Microbiol.*, 2012, **86**, 1334–1344.
43 A. F. van Peer, W. H. Müller, T. Boekhout, L. G. Lugones and H. A. B. Wösten, *PLoS One*, 2009, **4**, e5977.
44 A. Vinck, C. De Bekker, A. Ossin, R. A. Ohm, R. P. deVries and H. A. Wösten, *Environ. Microbiol.*, 2011, **13**, 216–225.
45 C. de Bekker, O. Bruning, M. J. Jonker, T. M. Breit and H. A. Wösten, *Genome Biol.*, 2011, **12**, R71.
46 A. Brand, J. D. Barnes, K. S. Mackenzie, F. C. Odds and N. A. Gow, *FEMS Microbiol. Lett.*, 2008, **287**, 48–55.
47 J. F. Toljander, V. Artursson, L. R. Paul, J. K. Jansson and R. D. Finlay, *FEMS Microbiol. Lett.*, 2006, **254**, 34–40.
48 V. Bianciotto, S. Andreotti, R. Balestrini, P. Bonfante and S. Perotto, *Eur. J. Histochem.*, 2001, **45**, 39–49.
49 M. T. Brandl, M. Q. Carter, C. T. Parker, M. R. Chapman, S. Huynh and Y. Zhou, *PLoS One*, 2011, **6**, e25553.
50 R. J. Silverman, A. H. Nobbs, M. M. Vickerman, M. E. Barbour and H. F. Jenkinson, *Infect. Immun.*, 2010, **78**, 4644–4652.
51 J. Dijksterhuis, M. Sanders, L. G. Gorris and E. J. Smid, *J. Appl. Microbiol.*, 1999, **86**, 13–21.
52 D. A. Hogan and R. Kolter, *Science*, 2002, **296**, 2229–2232.
53 N. Vanittanakom, W. Loeffler, U. Koch and G. Jung, *J. Antibiot.*, 1986, **39**, 888–901.
54 R. Maget-Dana and F. Peypoux, *Toxicology*, 1994, **87**, 151–174.
55 L. Kalai-Grami, I. Ben Slimane, M. Mnari-Hattab, S. Rezigui, M. A. Aouani, M. R. Hajlaoui and F. Limam, *World J. Microbiol. Biotechnol.*, 2013, **30**, 529–538.
56 D. Vitullo, A. Di Pietro, A. Romano, V. Lanzotti and G. Lima, *Plant Pathol.*, 2012, **61**, 689–699.
57 M. M. Nakano, N. Corbell, J. Besson and P. Zuber, *Mol. Gen. Genet.*, 1992, **232**, 313–321.
58 D. Lopez, M. A. Fischbach, F. Chu, R. Losick and R. Kolter, *Proc. Natl. Acad. Sci. U. S. A.*, 2009, **106**, 280–285.
59 P. Zhao, C. Quan, Y. Wang and S. Fan, *J. Basic Microbiol.*, 2014, **54**, 448–456.
60 H. Inoue, H. Nojima and H. Okayama, *Gene*, 1990, **96**, 23–28.
61 M. A. Wälti, C. Villalba, R. M. Buser, A. Grünler, M. Aebi and M. Künzler, *Eukaryotic Cell*, 2006, **5**, 732–744.
62 S. Swamy, I. Uno and T. Ishikawa, *J. Gen. Microbiol.*, 1984, **130**, 3219–3224.
63 J. D. Granado, K. Kertesz-Chaloupkova, M. Aebi and U. Kües, *Mol. Gen. Genet.*, 1997, **256**, 28–36.
64 T. J. Gryczan, S. Contente and D. Dubnau, *J. Bacteriol.*, 1978, **134**, 318–329.
65 D. C. Duffy, J. C. McDonald, O. J. A. Schueller and G. M. Whitesides, *Anal. Chem.*, 1998, **70**, 4974–4984.
66 J. Schindelin, I. Arganda-Carreras, E. Frise, V. Kaynig, M. Longair, T. Pietzsch, S. Preibisch, C. Rueden, S. Saalfeld, B. Schmid, J.-Y. Tinevez, D. J. White, V. Hartenstein, K. Eliceiri, P. Tomancak and A. Cardona, *Nat. Methods*, 2012, **9**, 676–682.

Downloaded from https://academic.oup.com/ib/article-abstract/6/10/935/5199045 by ETH Zürich user on 21 February 2019